Journal of the Anatomical Society of India 67 (2018) 115–119

Contents lists available at ScienceDirect

Journal of the Anatomical Society of India

journal homepage: www.elsevier.com/locate/jasi

Original Article

An anatomical study of the caprine posterior cruciate ligament

Yong Qin, Bin Zhang, Chao Huang, Song-Cen Lv*

Department of Orthopaedics, Second Affiliated Hospital of Harbin Medical University, Harbin, Heilongjaing Province, 150086, China

ARTICLE INFO

Article history:
Received 28 September 2018
Accepted 6 November 2018
Available online 10 November 2018

Keywords:
Posterior cruciate ligament
Anatomy
Anterolateral bundle
Posteromedial bundle
Sheep

ABSTRACT

Introduction: The pathophysiology and treatment techniques for posterior cruciate ligament (PCL) injuries and diseases are currently controversial and leave much room for improvement. However, the caprine PCL anatomy is not well known.
Methods: Forty-three caprine knees without degenerative or traumatic changes were studied.
Results: The passive range of motion was $42.1 \pm 9.0°$to $145.0 \pm 8.3°$for the caprine knee. The PMB was tighter than the ALB at the most extended angle of the knee. As the knee became flexed, the ALB became taut whereas the PMB was first relaxed and then taut. The insertion area of the ALB was 43.6 ± 9.3 mm^2 in the femur and 23.2 ± 5.1 mm^2 in the tibia, respectively. And that of the PMB was 19.1 ± 4.6 mm^2 and 39.6 ± 8.6 mm^2, respectively. The distance between the insertion centers of the two bundles was 7.23 ± 0.29 mm on the femur and 5.67 ± 0.69 mm on the tibia.
Discussion: Quantitative data on the size and morphology of the PCL anatomy were obtained on caprine knees, which provides guidance for future translational research on the sheep model to improve surgical techniques for surgical reconstruction and other PCL treatments.

1. Introduction

The posterior cruciate ligament (PCL) is located in the back of the knee. It is one of several ligaments that connect the femur to the tibia and it provides the primary restraint to posterior tibial translation. Injuries to the PCL are more difficult to evaluate than other ligament injuries in the knee, and the treatment methods have historically been controversial among the orthopedic community.[1] The most common treatment approaches include the two-root technique which makes two bundles of PCL, the anterolateral bundle (ALB) and the posteromedial bundle (PMB), and the inlay technique.[2–8]

However, the success of either technique varies widely from case to case. Part of the reason was a lack of understanding on the natural history and pathophysiology of the PCL injuries. In addition, for all surgical techniques, there also exist many unanswered questions regarding key factors such as the graft material and size as well as the tunnel placement. In this regard, translational research on animal models is a critical step towards gaining the understanding and refining the techniques. Such animal studies could provide practical and clinically relevant guidance on the human case when similar studies on human or even human cadavers are difficult to conduct due to ethics restrictions and lack of resources.[9] Among different animal models, large animals are advantageous because of their anatomical similarity to humans. Large animal models have also provided an experimental platform for development and evaluation of the efficacy and safety of novel treatments.[10]

Sheep serve as one kind of such experimental large animals for orthopedic studies, and have been proven useful in many past investigations.[11–16] From the human case we know that a better understanding of the anatomical structure of the two bundles of PCL is the basis of understanding the injuries and performing the surgical techniques.[17] However, to our best knowledge, there has been very little reported in the literature on the anatomy of the caprine PCL and no quantitative measurements are available for anterolateral and posteromedial bundle insertions to the femur and the tibia. Therefore, this study aims to perform a quantitative investigation on the anatomy of the caprine PCL. The anatomy information can then be used in future caprine experiments to optimize the outcomes of PCL reconstruction and when translating the sheep data to the human case.

2. Materials and methods

Forty-three caprine knees without observable degeneration or trauma were used for the investigation. Under the approval of the institutional animal ethics committee of Second Affiliated Hospital of Harbin Medical University, the caprine knees were purchased from a legal slaughterhouse. The knee joint was visually inspected

* Corresponding author.
E-mail address: lvsongcen@sina.com (S.-C. Lv).

https://doi.org/10.1016/j.jasi.2018.11.009
0003-2778/

on every knee to ensure there was no gross degenerative or traumatic changes that would have disrupted the PCL or its normal anatomical relationships. There was also no evidence of osteophytes, articular wear, or meniscal tears in the knees. The mean age of the knees was 12 months and all knees had passed the osteoepiphysis stage. All knees were frozen at the time of collection and maintained at $-20\,^{\circ}$C until the time of analysis. Before dissection, the knees were thawed overnight and placed on an upright stand.

For analysis, the passive range of motion of each knee was first measured using a goniometer with 1° gradation. The arms of the goniometer were aligned with the femoral and tibial shafts. The center of the goniometer was placed over the axis of rotation. All angles were measured relative to the neutral 0° defined as the complete extension of the femoral shaft. The experiment was repeated 3 times to ensure the reliability of the measurement results.

Following the range of motion measurements, the surrounding skin, muscle and capsule of the knees were removed while leaving the intra-articular structures intact. The synovial covering of the PCL was also carefully removed. The two bundles of the PCL, the anterolateral bundle (ALB) and the posteromedial bundle (PMB), were identified according to their tension and fiber orientation at varying knee flexion angles. Alternatively, using a natural gap of about 2–4 mm depth and 3 mm width dividing the two bundles near the insertion in the tibia, the ALB and PMB were also identified. The results of the above two methods to divide the PCL were cross-checked with each other to assess consistency.

Subsequently, the tension of each of the two bundles was tested using two bands. As shown in Fig. 1, the red band was used to pull the PMB, and the blue one to pull the ALB. By pulling the bands tethered in the middle of the two bundles away laterally, the tension was estimated and compared at different knee flexion angles in 10-degree intervals.

Following the tension test, the soft tissues were removed except for the femoral and tibial footprints of the PCL. To acquire a perfect sample of the femoral attachments of the PCL, the lateral femoral condyle was removed with an oscillating saw between the insertions of the anterior cruciate ligament and the PCL prior to division. Subsequently, the outlines of the anterolateral and posteromedial bundle footprints were marked with an electrodrill and a pencil. Following the marks, the bundles were completely abraded from the bone. For consistency, all dissections and markings were performed by a single orthopedic surgeon.

High-resolution digital images with a consistent predefined setting were acquired for all samples using a tripod-mounted digital camera (D70, Nikon Corp, Tokyo, Japan). To ensure the measurement accuracy, all images were calibrated by including a coin of 20 mm diameter next to the sample in the same plane of the maximum surface area of the footprint. The coin and the to-be-measured footprint were carefully positioned in the same plane and checked with a level as shown in Fig. 2. All images were imported into an image analysis software, ImageJ, to calculate the areas of insertion footprints and the distance between the footprint centers between the two bundles on both femur and tibia. The pixel dimension of each image used for calculation was then calibrated using the coplanar coin on the image based on its known size.

3. Results

The passive range of caprine knee motion was $42.1 \pm 9.0^{\circ}$to $145.0 \pm 8.3^{\circ}$. Unlike human knees that fully extend at 0°, the most extension of caprine knees was at about 40°. At this most extended angle, the PMB was tighter than the ALB. As the caprine knee became flexed, the ALB gradually became more taut whereas the PMB first became more relaxed and then taut.

The anterior and posterior views of the caprine knee and the cruciate ligament (Fig. 3a–d), as well as the posterior view and the cleft between the two bundles of the PCL (Fig. 3e–f) are shown in Fig. 3, as obtained at the different stages of dissection as described in the Methods section. As shown in Fig. 3f, a cleft of about 2–4 mm depth and 3 mm width naturally divides the ALB and the PMB near the insertion in the tibia.

For the insertion area measurement, it was important to ensure that the coin used for scale calibration was coplanar with the insertion footprint to be measured. For the caprine knee, the relative positioning of the insertion footprints of the two bundles was different on the femur versus on the tibia. On the tibia, the insertion footprints of the two bundles are coplanar, so a single image could be acquired for the area measurement of both bundles. But because on the femur the insertion footprints of the two bundles were not coplanar but approximately perpendicular to each other, three images were acquired for the femoral insertion sites, including one image at about 45° angle to both footprints for calculating the distance between the two footprint centers, and

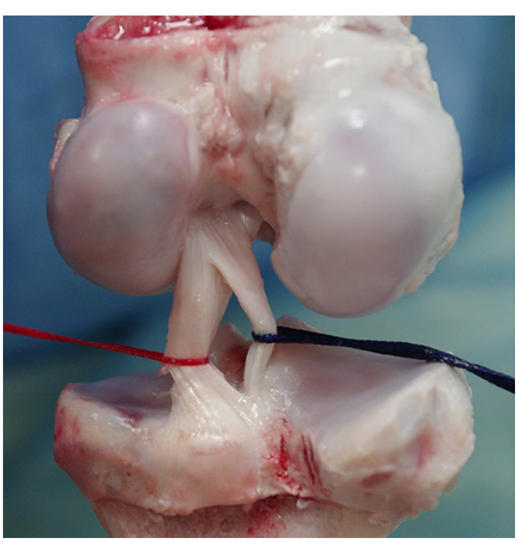

Fig. 1. Experimental setup for the bundle tension test at different knee flexion angles. As shown, using the red band to pull the PMB, and the blue band to pull the ALB, the relative tension of the two bundles was compared at different knee flexion angles between the most extended and the most flexed angles.

Fig. 2. An example digital image for the bundle insertion footprint surface area measurement. For scale calibration, a coin (diameter = 20 mm) was placed next to the footprint with the coin positioned in the same plane with the footprint, verified with a level. The image was also marked with the sample number (knee #13 in the example).

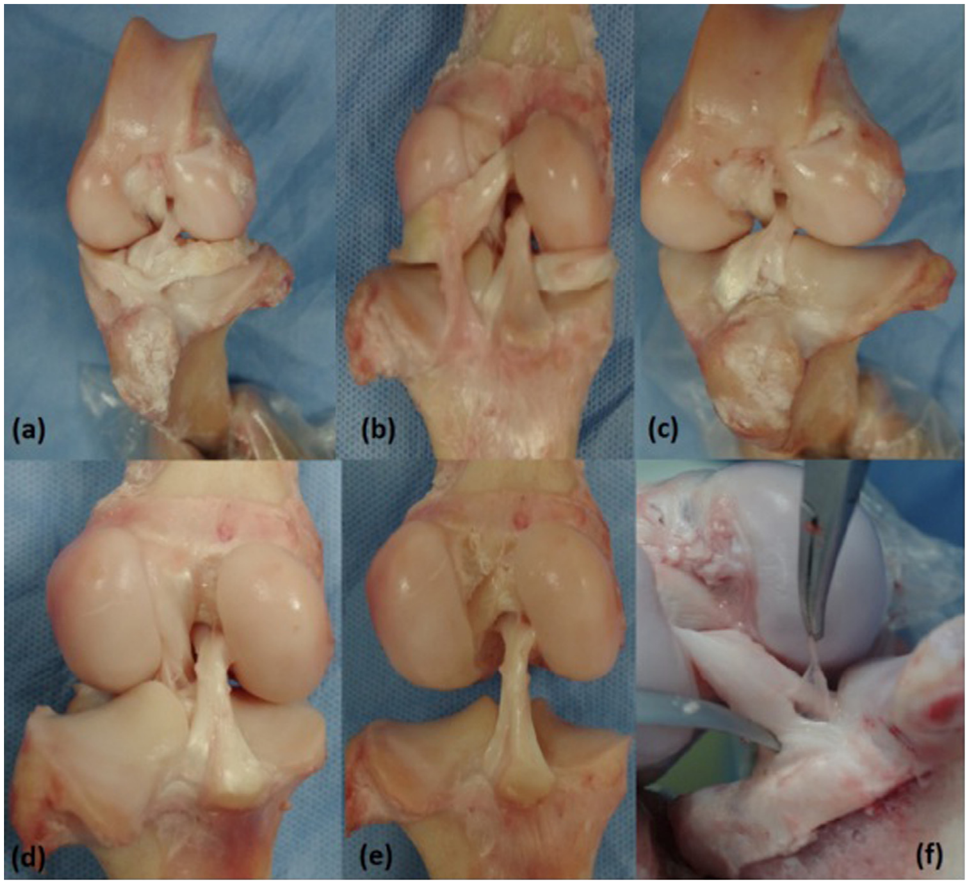

Fig. 3. Anatomical views of the caprine knee: (a) the anterior view of the whole knee, (b) the posterior view of the whole knee, (c) the anterior view of the cruciate ligament, (d) the posterior view of the cruciate ligament, (e) the posterior view of the PCL, and (f) the cleft naturally dividing the ALB and the PMB near the tibia.

two others each acquired *en face* to one footprint surface with the coin coplanar to measure the maximum area. An example image is shown in Fig. 4 in which the coin was aligned to be coplanar with the ALB.

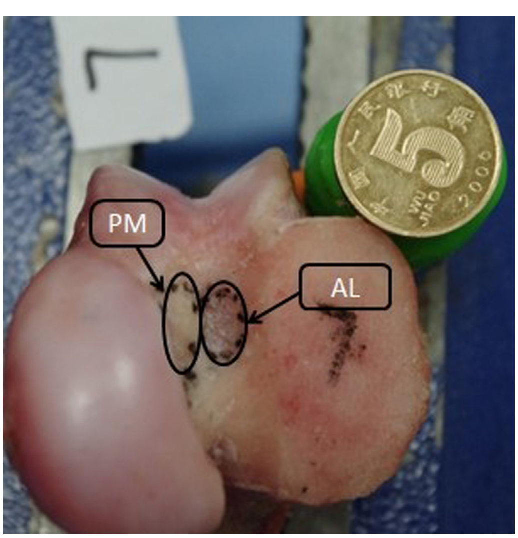

Fig. 4. An example image showing the coin aligned coplanar with the ALB footprint for the ALB femoral insertion footprint surface area measurement. A different image was acquired with the coin coplanar with the PMB footprint to measure the PMB footprint area and a third image was acquired along the diagonal plane between the two bundle surfaces to measure the footprint center distance.

The average surface areas of the PCL femoral and tibial insertion footprints are shown in Table 1. The distance between the centers of the two bundles on the femur and tibia was 7.23 ± 0.29 mm and 5.67 ± 0.69 mm, respectively.

4. Discussion

Knowledge of the biomechanical function of the native PCL and its individual bundles provides a framework for the understanding of the kinematic function in both the isolated PCL-deficient knee and in the multiligament injury state.[18] However, the natural history of the PCL injuries has yet to be elucidated fully and the surgical techniques for repair also leave much room for improvement. Animal models, especially those of large animals, play a key role in the ongoing research to understand the pathophysiology and to develop and refine the treatment techniques for PCL injuries. Sheep has been one such important animal model.[11–16] For example, Scheffler et al. conducted a key study using 48 sheep to compare allografts and autografts for anterior cruciate ligament reconstruction.[16]

At the same time, it is important to note that although the anatomy of large animal models like sheep is markedly similar to that of humans than the small animal models, there still exist some

Table 1
Average surface area (in mm^2) of the caprine PCL attachments (insertion footprints) to the femur and tibia.

	Overall	ALB	PMB
Femur	63.73 ± 14.35	43.61 ± 9.34	19.09 ± 4.65
Tibia	62.81 ± 10.89	23.23 ± 5.07	39.58 ± 8.58

anatomic differences. In our study we found a passive motion range of caprine knees from about 42° to about 145°. While the largest flexion at 145° resembles that of human knees, the sheep model couldn't reach a neutral 0° angle whereas the human knee could be brought to full extension. This result was in agreement with previous findings.[21] It is crucial to keep this difference in mind when translating sheep data to the human case.

Previous anatomic studies have mechanically characterized the individual bundles of the human PCL, showing that the normal ALB is more taut in flexion and more lax in extension.[19],[20] The reverse is true for the human PMB that it is relatively more taut in extension and more lax in flexion. Whereas for the sheep model, we observed that while the caprine ALB behaves in the same way as the human ALB, the caprine PMB first become more lax but then become taut in flexion. Although we did not quantify the tension during this experiment, the above qualitative finding was verified with repeat experiments and on different caprine knees.

Qualitative topographic assessment and quantitative surface area measurement of the ALB and PMB footprints are important to improve the currently varying success of PCL reconstruction. The accurate characterization of the location and size of the two bundles of the PCL on the femur and tibia is necessary for the accurate placement determination of femoral and tibial tunnels, therefore ultimately crucial for the outcomes of reconstructive surgery. There have been a large body of literature investigating and reporting on these measurements for the human PCL.[22–27]

These human investigations were conducted using human cadaveric knees. To compare with the caprine knee results obtained in our study, we summarized the human knee results in Table 2 from the femoral investigations by Forsythe et al. and Lopes et al. and the tibial investigation by Tajima et al. [24–26] From those studies, the center distance between the two bundles from these studies was 11 ± 1.18 mm for the femoral attachments and 8.2 ± 1.3 for the tibial attachments, respectively. The data were summarized from studies by Forsythe et al., Lopes et al., and Tajima et al. [24–26]

Compared with human knees, the caprine PCL bundles were found to have smaller surface areas and smaller bundle center distances in our study. Also, while the insertion sites of the two bundles were found to locate in different planes for both tibia and femur in human knees, the insertion sites for caprine tibia were found to be relatively coplanar in our study. To our knowledge, this is the first time the morphology and quantitative measurements of the PCL anatomy have been reported for the sheep model. These results will be critical to optimize the techniques and outcomes for surgical reconstruction experiments on sheep, and to translate existing and future caprine data to the human case.

There also exist some variations in different literatures on area measurements of the human PCL bundle attachments in addition to the results summarized in Table 2. For example, Takahashi et al. reported areas of the ALB and the PMB in the femur of 58.0 ± 25.4 and 64.6 ± 24.7 mm^2 and those in the tibia of 46.7 ± 15.6 and 115.8 ± 54.6 mm^2 [27]. Luo et al. reported femoral footprint areas of 78.53 ± 28.38 mm^2 for the ALB and 72.71 ± 28.39 mm^2 for the PMB, and tibial footprint areas of 83.99 ± 23.29 and 76.01 ± 15.76 mm^2, respectively.[22] Contributing to these variations were multiple factors. Because these human studies were all performed on cadaveric knees, traumatic or degenerative changes on some knees could have contributed some uncertainties. In contrast, the current caprine study selected knees all of the same age and free of any traumatic or degenerative change. Another big variation among the human studies was the methods using which the footprint area measurements were made. Due to the complex shape and orientation of the footprint, the measurement could have large uncertainties. In our study, measurements were made on digital images using image processing and analysis software, which largely ensured the objectivity and improved the accuracy of the measurements. In addition, during the image acquisition, the coin used for pixel size calibration was carefully positioned in the same plane as the footprint and verified with a level to maximize the accuracy of the measurement.

As a future direction to extend the current research, the replacement grafts can be investigated for the caprine PCL, by determining the kinematic contribution of the bundles as well as the *in situ* forces in them in response to various external loading conditions. Histology can also be studied to compare with the human PCL.

Table 2
Average surface area (in mm^2) of the human PCL attachments to the femur and tibia.

	Overall	ALB	PMB
Femur	209 ± 33.82	118 ± 23.95	90 ± 16.13
Tibia	243.9 ± 38.2	93.1 ± 16.6	150.8 ± 31.0

5. Conclusion

In Conclusion similar to the human PCL, the caprine PCL also consist of a complex fibrous architecture that can be functionally divided into 2 components, the ALB and the PMB, with each component having specific insertions. In this study, we have provided a visualization of the 2-dimensional shapes as well as the quantitative measurements of these insertions. This information on the specific insertion site areas and geometry can aid in tunnel placement for both single- and double-bundle reconstructive techniques on the sheep model and for future translation of the caprine data to the human case.

Conflict of interest

None.

References

1. Fanelli GC, Beck JD, Edson CJ. Single compared to double-bundle PCL reconstruction using allograft tissue. *J Knee Surg*. 2012;25:59–64.
2. Christel P. Basic principles for surgical reconstruction of the PCL in chronic posterior knee instability. *Knee Surg Sports Traumatol Arthrosc*. 2003;11:289–296.
3. Dowd GS. Reconstruction of the posterior cruciate ligament. Indications and results. *J Bone Joint Surg Br*. 2004;86:480–491.
4. Harner CD, Fu FH, Irrgang JJ, Vogrin TM. Anterior and posterior cruciate ligament reconstruction in the new millennium: A global perspective. *Knee Surg Sports Traumatol Arthrosc*. 2001;9:330–336.
5. Höher J, Scheffler S, Weiler A. Graft choice and graft fixation in PCL reconstruction. *Knee Surg Sports Traumatol Arthrosc*. 2003;11:297–306.
6. Mariani PP, Becker R, Rihn J, Margheritini F. Surgical treatment of posterior cruciate ligament and posterolateral corner injuries. An anatomical, biomechanical and clinical review. *Knee*. 2003;10:311–324.
7. Miller MD, Cooper DE, Fanelli GC, Harner CD, LaPrade RF. Posterior cruciate ligament: Current concepts. *Instr Course Lect*. 2002;51:347–351.
8. Wind [42_TD$DIFF]Jr WMJr, Bergfeld JA, Parker RD. Evaluation and treatment of posterior cruciate ligament injuries: Revisited. *Am J Sports Med*. 2004;32:1765–1775.
9. Arnoczky SP, Cook JL, Carter T, Turner AS. Translational models for studying meniscal repair and replacement: What they can and cannot tell us. *Tissue Eng Part B Rev*. 2010;16:31–39.
10. Reinwald S, Burr D. Review of nonprimate, large animal models for osteoporosis research. *J Bone Miner Res*. 2008;23:1353–1368.
11. Meller R, Kendoff D, Hankemeier S, et al. Hindlimb growth after a transphyseal reconstruction of the anterior cruciateligament: A study in skeletally immature sheep with wide-open physes. *Am J Sports Med*. 2008;36:2437–2443.
12. Gupte CM, Bull AM, Murray R, Amis AA. Comparative anatomy of the meniscofemoral ligament in humans and some domestic mammals. *Anat Histol Embryol*. 2007;36:47–52.
13. Bosch Ulrich, Decker Brigitte, Kasperczyk Werner, Nerlich Andreas, Oestern Hans-Joerg, Tscherne Harald. The relationship of mechanical properties to

morphology in patellar tendon autografts after posterior cruciate ligament replacement in sheep. *J Biomech*. 1992;25(8):821–830.

14. Bosch U, Kasperczyk WJ, Decker B, Oestern HJ, Tscherne H. The morphological effects of synthetic augmentation in posterior cruciate ligament reconstruction an experimental study in a sheep model. *Arch Orthop Trauma Surg*. 1996;115(3-4):176–181.
15. Kasperczyk WJ, Bosch U, Oestern HJ, Tschcerne H. Influence of immobilization on autograft healing in the knee joint. A preliminary study in a sheep knee PCL model. *Arch Orthop Trauma Surg*. 1991;110:158–161.
16. Scheffler SU, Schmidt T, Gangéy I, Dustmann M, Unterhauser F, Weiler A. Fresh-frozen free-tendon allografts versus autografts in anterior cruciate ligament reconstruction: Delayed remodeling and inferior mechanical function during long-term healing in sheep. *Arthroscopy*. 2008;24(4):448–458.
17. Luo H, Ao YF, Zhang WG, Liu SY, Zhang JY, Yu JK. Anatomical study of the anterolateral and posteromedial bundles of the posterior cruciate ligament for double-bundle reconstruction using the quadruple bone-tunnel technique. *Chin Med J*. 2012;125(22):3972–3976.
18. Voos JE, Mauro CS, Wente T, Warren RF, Wickiewicz TL. Posterior cruciate ligament : Anatomy, biomechanics, and outcomes. *Am J Sports Med*. 2012;40:222–231.
19. Girgis FG, Marshall JL, Monajem A. The cruciate ligaments of the knee joint. Anatomical, functional and experimental analysis. *Clin Orthop Relat Res*. 1975;106:216–231.
20. Van Dommelen BA, Fowler PJ. Anatomy of the posterior cruciate ligament: A review. *Am J Sports Med*. 1989;17(1):24–29.
21. Proffen BL, McElfresh M, Fleming BC, Murray MM. A comparative anatomical study of the human knee and six animal species. *Knee*. 2012;19:493–499.
22. Harner CD, Baek GH, Vogrin TM, Carlin GJ, Kashiwaguchi S, Woo SL. Quantitative analysis of human cruciate ligament insertions. *Arthroscopy*. 1999;15:741–749.
23. Luo H, Ao YF, Zhang WG, Liu SY, Zhang JY, Yu JK. Anatomical study of the anterolateral and posteromedial bundles of the posterior cruciate ligament for double-bundle reconstruction using the quadruple bone-tunnel technique. *Chin Med J*. 2012;125(22):3972–3976.
24. Forsythe B, Harner C, Martins CA, Shen W, Lopes Jr OVJr. Topography of the femoral attachment of the posterior cruciate ligament: Surgical technique. *e Joint Surg Am*. 2009;91(Suppl. 2) Pt1:89-100.
25. Lopes Jr OVJr, Ferretti M, Shen W, Ekdahl M, Smolinski P, Fu FH. Topography of the femoral attachment of the posterior cruciate ligament. *J Bone Joint Surg Am*. 2008;90(2):249–255.
26. Tajima G, Nozaki M, Iriuchishima T, et al. Morphology of the tibial insertion of the posterior cruciate ligament. *J Bone Joint Surg Am*. 2009;91(4):859–866.
27. Takahashi M, Matsubara T, Doi M, Suzuki D, Nagano A. Anatomical study of the femoral and tibial insertions of the anterolateral and posteromedial bundles of human posterior cruciate ligament. *Knee Surg Sports Traumatol Arthrosc*. 2006;14(November (11)):1055–1059.